High Throughput Functional Analysis of *KCNB1* variants Associated with Epileptic Encephalopathy Type 26

Jennifer A. Kearney[1], Carlos G. Vanoye[1], Jeffrey Calhoun[1], Dianalee McKnight[2], Laurie Demmer[3], Paula Goldenberg[4], Lauren E. Grote[5], Kevin Strauss[6], Ali Torkamani[7], Jasper van de Smagt[8], Alfred L. George, Jr. [1]

[1]Department of Pharmacology, Northwestern University Feinberg School of Medicine, [2]GeneDX, [3]Department of Pediatrics, Carolinas Medical Center, [4]Mass General Hospital for Children, [5]Division of Clinical Genetics, Children's Mercy Hospital, University of Missouri-Kansas City School of Medicine, [6]Clinic for Special Children, [7]Scripps Translational Science Institute and Scripps Research Institute, [8]Department of Medical Genetics, University Medical Center Utrecht

Background and Rationale

Mutations in *KCNB1* have recently been implicated as the cause of epileptic encephalopathy type 26 (EIEE26) [1-3]. EIEE26 is characterized by multifocal seizures, global developmental delay, and hypotonia. *KCNB1* encodes the Kv2.1 voltage-gated potassium channel alpha subunit, which is a major contributor to delayed rectifier potassium current in the brain. We previously demonstrated pathogenic effects of three EIEE26-associated *KCNB1* mutations (S347R, T374I, G379R) on Kv2.1 protein function. CHO-K1 cells expressing the mutant channels exhibited loss of ion selectivity and voltage-dependent gating, and gain of a depolarizing inward cation conductance [1]. Similarly, a recent report of a novel EIEE26 mutation also demonstrated loss of ion selectivity and gain of a depolarizing cation conductance as major effects [3]. However, they did not observe loss of voltage-dependent gating. This suggests that a range of channel dysfunction can result in EIEE26 with similar clinical features. To define the range of mutation effects, we studied a series of six variants from cases with a molecular diagnosis of EIEE26 ascertained by clinical exome sequencing.

Study Subjects

Patients were referred for clinical exome sequencing for epileptic encephalopathy or global developmental delay of unknown cause. De-identified clinical summaries and genetic results were collected. Patients ranged in age from 3-20 years. All subjects had abnormal EEG most often characterized by multifocal spike discharges and background slowing. Seizure onset is in late infancy to early childhood and frequently begins with focal dyscognitive seizures that may initially go unrecognized. Additional seizure types may emerge, including myoclonic, atonic, and generalized tonic-clonic (GTC). Seizures are refractory to treatment. Other associated phenotypes include hypotonia, ataxia, and intellectual disability.

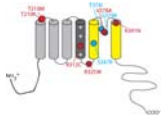

Location of KCNB1 mutations on Kv2.1 primary structure. New variants are shown in read. Previously characterized variants are shown in blue [1].

Methods

To determine the effect of these *KCNB1* variants on Kv2.1 channel function, we performed functional studies in a heterologous expression system. *KCNB1* variants were introduced into a full-length human Kv2.1 cDNA expression construct by site-directed mutagenesis. Expression of wild-type (WT) or mutant Kv2.1 in CHO-K1 cells was achieved by electroporation. Following 72 hour recovery, automated planar array patch clamp recording was performed. Only cells with $R_{seal} \geq 0.5G\Omega$, $R_{series} \leq 15M\Omega$ and $I_{peak}/I_{late} \leq 1$ were used for analysis. Cell surface biotinylation experiments were performed to determine the relative expression of WT and mutant channel protein at the plasma membrane.

Figure 1. High throughput Analysis of KCNB1

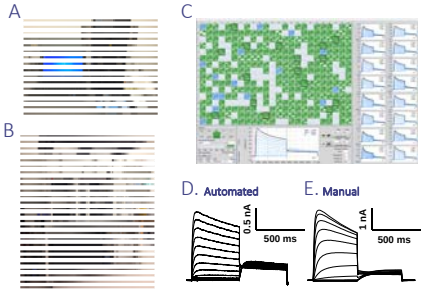

Figure 1. High throughput analysis of *KCNB1* variants associated with epilepsy was achieved by transient transfection of CHO-K1 cells with wild type or mutant Kv2.1 cDNAs using the MaxCyte STX electroporation system (**A**) followed by functional analysis with the SyncroPatch 384 (**B**). A screen shot of a typical experiment is shown in panel **C** with 16 individual cell recordings depicted in the right side. An averaged whole-cell recording from cells expressing Kv2.1 (**n=53**) obtained with the SyncroPatch is shown in **D**. Peak currents were recorded during 500 ms long depolarizing steps from -80 to +60 mV followed by a 500 ms step to 0 mV (tail currents). The holding potential was -80 mV. Whole-cell recording from CHO-K1 cells expressing wild type Kv2.1 obtained by manual patch using an identical voltage-protocol is shown in **E** (Torkami *et al*, 2014).

Figure 2. Functional Analysis of KCNB1 Variants

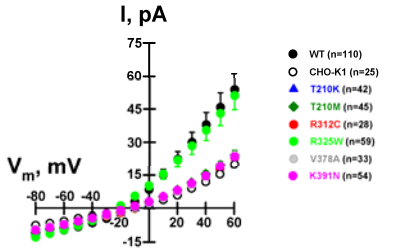

Figure 2. Average current- voltage (IVs) relationships are shown for the whole-cell currents recorded from non-transfected CHO-K1 cells or cells transiently expressing homomeric wild-type (WT) or variant Kv2.1 channels. Only the R325W variant exhibited sizeable currents while all the other variants were indistinguishable from non-transfected cells. The currents are normalized to membrane capacitance and shown as mean and SEM for clarity. The number of cells (n) for each variant are listed in the figure.

Figure 3. R325W Alters Voltage-Dependence

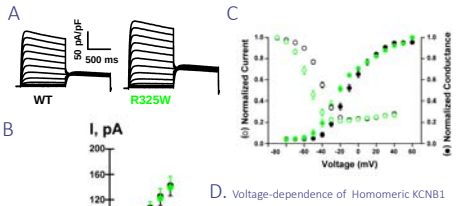

D. Voltage-dependence of Homomeric KCNB1 Channels

	Activation		Inactivation	
	V½	k	V½	k
WT	-10.6 ± 1.8	11.5 ± 0.5(n=51)	-42.5 ± 1.1	7.0 ± 0.3(n=35)
R325W	-21.4 ± 1.9*	17.1 ± 1.5*(n=21)	-56.1 ± 1.8*	6.0 ± 0.3†(n=25)

Figure 3. **A.** Averaged whole-cell currents recorded from cells expressing homomeric WT (**n=53**) or R325W (**n=23**) Kv2.1 channels. **B.** Average voltage-current relationships measured from the currents shown in **A** for WT (●) and R325W (●) channels. The currents are normalized to membrane capacitance and shown as mean and SEM for clarity. **C.** Activation and inactivation curves were obtained from tail currents and by a 5 s long pre-pulses from -90 to +40 mV followed by 250 ms step to +60 mV. **D.** Voltage-dependence parameters were obtained by Boltzmann fits to activation and inactivation curves. * = P<0.005, † = P <0.05.

Figure 4. Analysis of Heteromeric KCNB1 Channels

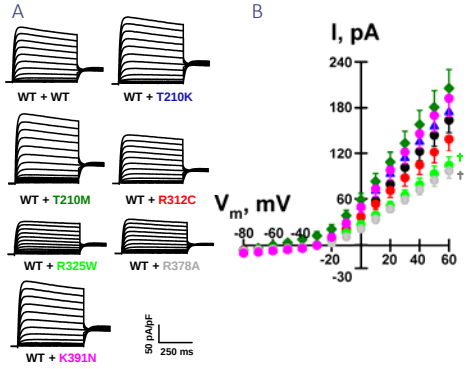

Figure 4. **A.** Averaged whole-cell currents recorded from cells expressing WT + variant heteromeric Kv2.1 channels. **B.** Average voltage-current relationships measured from the currents shown in **A** for WT+WT (●, **n=53**), WT+T210K (▲, **n=35**), WT+T210M (◆, **n=33**), WT+R312C (●, **n=34**), WT+R325W (●, **n=31**), WT+R378A (●, **n=25**) and WT+K391 (●, **n=34**), channels. The currents are normalized to membrane capacitance and shown as mean and SEM for clarity. † = P <0.05

Figure 5. Activation and Inactivation of Het KCNB1 Channels

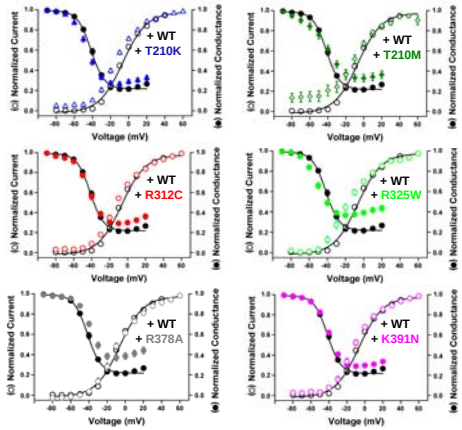

Figure 5. Activation (open symbols) and inactivation (solid symbols) curves obtained from WT + variant heteromeric Kv2.1 channels. Data were fit with the Boltzmann equation .

Table2. Voltage-dependence of Het KCNB1 Channels

	Activation		Inactivation	
	V½	k	V½	k
WT+WT	-8.4 ± 1.1	11.2 ± 0.3 (n=53)	-40.8 ± 1.1	5.6 ± 0.1(n=38)
WT+T210K	-13.7 ± 1.1*	12.3 ± 0.3(n=35)	-47.0 ± 1.1*	6.0 ± 0.2(n=35)
WT+T210M	-9.2 ± 1.9	12.0 ± 0.9(n=28)	-39.1 ± 1.6	6.8 ± 0.3*(n=21)
WT+R312C	-11.7 ± 1.3	12.4 ± 0.4(n=29)	-43.6 ± 1.2	5.8 ± 0.2(n=30)
WT+R325W	-17.8 ± 3.1*	12.8 ± 1.1(n=18)	-51.0 ± 1.4*	5.5 ± 0.1(n=29)
WT+V378A	-8.5 ± 1.6	13.7 ± 0.6*(n=23)	-38.9 ± 1.1	4.9 ± 0.2*(n=26)
WT+K391N	-11.6 ± 1.4	11.6 ± 0.4(n=33)	-40.5 ± 0.9	5.7 ± 0.2(n=42)

* = P<0.005

Figure 6. Reduced Expression and/or Trafficking

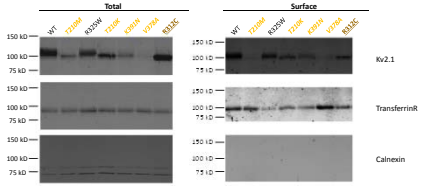

- *Reduced cell surface and total expression*
- **Reduced trafficking**

Figure 5. Cell surface expression was measured using cell surface biotinylation of CHO-K1 cells electroporated with wild-type (WT) or mutant Kv2.1. Total and surface fractions were detected with a mouse monoclonal anti-Kv2.1 antibody (Neuromab, ASC-003; 1:250). Endogenous transferrin receptor (TransferrinR) levels were measured as a loading control with a mouse monoclonal antibody (Invitrogen, #13-6800; 1:500). Endogenous calnexin levels were measured as a control for cell surface labeling using a polyclonal antibody (Santa Cruz Biotech, H70; 1:250). Calnexin immunoreactivity was consistently absent from surface fractions as expected. Blot shown is representative of three independent experiments.

Summary

- EIEE26 presents in infancy with multiple seizure types, developmental delay, hypotonia, and movement disorders.
- All *KCNB1* mutations described to date have arisen de novo.
- Functional studies demonstrate that *KCNB1* mutations associated with epileptic encephalopathy result in a spectrum of effects that result in lower activity and/or altered voltage-dependence of activation and inactivation.
- Future studies will test whether the mutations affect ion channel selectivity
- Restoration of Kv2.1 function may be therapeutic

References

1. Torkamani A, et al (2014) De novo KCNB1 mutations in epileptic encephalopathy. Ann Neurol. 76(4):529-40.
2. Saitsu H, et al (2015) De novo KCNB1 mutations in infantile epilepsy inhibit repetitive neuronal firing. Sci Rep. 5:15199.
3. Thiffault I, et al (2015) A novel epileptic encephalopathy mutation in KCNB1 disrupts Kv2.1 ion selectivity, expression, and localization. J Gen Physiol. 146:399-410.
4. Speca DJ, et al (2014) Deletion of the Kv2.1 delayed rectifier potassium channel leads to neuronal and behavioral hyperexcitability. Genes Brain Behav.13:394-408.

Supported by

NIH grants R01-NS053792 (J.A.K.) and R01-NS032387 (A.L.G.)

Northwestern Medicine
Feinberg School of Medicine